Neutron and in Situ X-ray Investigation of Hydrogen Intake in Titanium-Based Cubic Alloys

M. Blouin and R. Schulz

Technologies Émergentes de Production et de Stockage, Institut de Recherche d'Hydro-Québec, 1800 Blvd. Lionel-Boulet, C.P. 1000, Varennes, Québec, Canada, J3X 1S1

M.-E. Bonneau, A. Bercier, L. Roué, and D. Guay*

INRS-Énergie et Matériaux, 1650 Blvd Lionel-Boulet, C.P. 1020, Varennes, Québec, Canada J3X 1S2

I. P. Swainson

Steacie Institute of Molecular Sciences, National Research Council, Chalk River Laboratories, Chalk River, Ontario, Canada K0J 1J0

Received May 13, 1999. Revised Manuscript Received September 8, 1999

The structure of nanocrystalline Ti:Ru:Fe $(2 - y):(1+ y)/2:(1 + y)/2)$ obtained by high-energy ball milling has been studied by X-ray and neutron diffraction as a function of the Ti content, for y varying from 0.00 to 1.00 by step of 0.25, using Rietveld refinement analysis. When $y = 0.00$, a nanocrystalline metastable B2 cubic phase is formed, with most of the 1a site occupied by Ti atoms and the 1b site occupied by either Fe or Ru atoms. When decreasing the Ti content, the B2 structure becomes less stable. A preferential replacement of Ti by Fe on the 1a occurs and leads to the precipitation of hcp Ru. In situ X-ray diffraction measurements under hydrogen at high pressure were also made. In all cases, a shift of the diffraction peaks of the B2 structure toward the smaller 2θ values was observed. This shift is totally reversible upon removing hydrogen. It indicates that hydrogen is absorbed into the materials. The volume increase of the B2 structure varies according to the Ti content, reflecting the fact that less hydrogen is absorbed when Ti is reduced. Assuming that the volume occupied by a single hydrogen atom is ∼2.5 D^3, the hydrogen content of the various nanocrystalline Ti:Ru:Fe $(2 - y):(1 + y)/2:(1 + y)/2)$ is calculated from the volume increase of the unit cell of the corresponding materials.

Introduction

In the past few years, mechanical alloying by high-intensity ball milling has been successfully applied to the synthesis of various materials. This method of material preparation has become an important field of research in material sciences and numerous applications are envisioned.[1,2] This holds particularly true in the field of electrocatalysis, where it was shown that considerable improvement in the electrocatalytic activity for hydrogen evolution in typical chlorate electrolysis conditions can be obtained by using nanocrystalline Ti_2RuFe alloy prepared by milling a powder mixture of Ti:Ru:Fe (2:1:1).[3]

During prolonged electrolysis, the nanocrystalline Ti:Ru:Fe (2:1:1) electrode suffers from decrepitation and loss of materials, which results in an increase of the cathodic overpotential and, eventually, to the destruction of the electrode.[4] This limitation can be overcome and the structural integrity of the electrode can be dramatically improved by the addition of oxygen. For example, the cathodic overpotential in typical chlorate electrolysis conditions of electrodes made from nanocrystalline materials obtained by milling Ti:Ru:Fe:O (2:1:1:2) does not vary over a period of 1000 h (the longest test conducted so far), nor does the electrode show any sign of degradation after this prolonged test.[5] For comparison, the cathodic overpotential of an electrode made from the O-free material starts to increase (becoming more cathodic) after only ∼100 h.[4] Obviously, oxygen has a beneficial effect on the stability of the electrode.

A first hint at the reasons underlying the improved stability caused by the addition of O comes from the markedly different behavior that both materials exhibit when they are subjected to a succession of cycles of hydrogen discharge and open circuit conditions. In experiments where the hydrogen discharge and open

* To whom correspondence should be sent. E-mail: guay@inrs-ener.uquebec.ca.

(1) Suryanarayana, C. *Bibliography on Mechanical Alloying and Milling*; Cambridge Interscience Publ.: Cambridge, UK, 1995.
(2) Koch, C. C.; Whittenberger, J. D. *Intermetallics* **1996**, *4*, 339.
(3) Blouin, M.; Guay, D.; Huot, J.; Schulz, R. *J. Mater. Res.* **1997**, *12*, 1492.
(4) Roué, L.; Irissou, É.; Bercier, A.; Bouaricha, S.; Blouin, M.; Guay, D.; Boily, S.; Huot, J.; Schulz, R. *J. Appl. Electrochem.* **1999**, *29*, 551.
(5) Van Neste, A.; Yip, S.-H.; Jin, S.; Boily, S.; Ghali, E.; Guay, D.; Schulz, R. *Mater. Sci. Forum* **1996**, *225−227*, 795.

10.1021/cm990293z CCC: $18.00
Published on Web 10/27/1999

circuit conditions last 10 min each, some material starts to fall from the surface of the Ti:Ru:Fe (2:1:1) electrode at the 10th cycle, leading to a marked increase of the cathodic overpotential at the 20th cycle.[4] In contrast, there is no change in the cathodic overpotential of the Ti:Ru:Fe:O (2:1:1:1) electrodes even after 50 cycles, nor does the surface of the electrode show any sign of material lost. To explain this different behavior, it was hypothesized[4] (i) that hydrogen is able to dissolve into the structure of the O-free nanocrystalline material during hydrogen discharge, while it is released from the electrode under open circuit conditions and (ii) that the structural changes associated with the dissolution/release of hydrogen into/from the material lead to the decrepitation and destruction of the electrode. Direct evidence of hydrogen intake and release can be achieved by performing in situ X-ray diffraction measurements under hydrogen at high pressure, with an eye for shift in the peak position as the lattice parameter expands upon hydrogen absorption. Such measurements will be presented in this study.

There is another issue that still needs some clarification: the structural and phase composition changes of nanocrystalline Ti:Ru:Fe (2:1:1) when oxygen is introduced in the structure. Some recent X-ray and neutron diffraction analyses of related materials[3,6−8] have established that prolonged milling of Ti:Ru:Fe (2:1:1) produces a nanocrystalline alloy made almost exclusively (97 wt %) of a B2 cubic phase (cP2−CsCl), whose composition is Ti_2RuFe, with only a small fraction (3 wt %) of iron, coming most probably from the erosion of the crucible and balls. At the opposite, the materials obtained after extensive milling of Ti:Ru:Fe:O (2:1:1:2) are *multiphased*, comprising ∼60 wt % of a B2 cubic phase, ∼30 wt % of titanium oxides, and the remaining 10 wt % being either Ru or Fe. In Ti:Ru:Fe:O (2:1:1:2), the ratio Ti/O is fixed at unity by the initial composition of the powder. Thus, the formation of stable titanium oxide phases during milling reduces the amount of Ti atoms involved in the formation of the less stable B2 cubic phase. This was shown through a detailed analysis of both X-ray and neutron diffraction data of a series of nanocrystalline Ti:Ru:Fe:O (2:1:1:*w*), where *w* was varied from 0 to 2.[7] In that study, it was demonstrated that the presence of oxygen in the powder mixture leads to the *formation of a Ti-depleted B2 cubic phase*, $Ti_{2-x}Ru_{1+y}Fe_{1+z}$, with *x* being as large as 0.74 when $w = 1.5$. On the basis of these structural differences, it was hypothesized[4,7] that the improved stability of the nanocrystalline Ti:Ru:Fe:O (2:1:1:2) materials could arise as a consequence of a *modification of the intrinsic hydrogen absorption properties of the Ti-depleted B2 cubic phase*. The study of materials made from "pure" Ti-depleted B2 cubic structure prepared without the addition of oxygen would obviously help to clarify this issue.

The purpose of this paper is 2-fold. First, we want to demonstrate that Ti-depleted B2 cubic phase of the general formula $Ti_{2-y}Ru_{(1+y)/2}Fe_{(1+y)/2}$ can be prepared by high-energy ball milling, starting from a powder mixture of Ti:Ru:Fe $(2 - y):(1 + y)/2:(1 + y)/2)$. Second, we want to demonstrate that there is a sizable increase in the volume of the unit cell of the B2 phase when it is exposed to H_2, thus giving support to the idea that absorption of hydrogen into the structure of the material during hydrogen discharge is in part responsible for the degradation of the electrode. To do so, in situ X-ray diffraction measurements at high hydrogen pressure will be performed. It will be shown that the volume expansion of the unit cell of the B2 cubic phase is highly dependent on composition. The consequence of this assertion on the markedly different stability behavior observed when O is added to nanocrystalline Ti:Ru:Fe (2:1:1) will be outlined.

Experimental Section

Samples were made by high-energy ball milling using a SPEX 8000 mixer/mill apparatus. On the basis of previous experiments,[3] the milling time was set at 40 h. In all cases, steel balls and vials were used. The vial had a diameter of 38.1 mm and a length of 47.6 mm. Three balls were used, one with a diameter of 14 mm and two with a diameter of 11 mm. The ball-to-powder ratio was about 4:1. In all cases, the vial was filled with argon to prevent oxidation and nitridation reactions.

Pure Ti, Ru, and Fe (>99.9%) powders were used as starting materials. The initial powder mixture Ti:Ru:Fe was $2 - y:(1 + y)/2:(1 + y)/2$, with *y* ranging from 0 to 1 by step of 0.25. The X-ray diffraction histograms of these samples were taken on a Philips X-PERT diffractometer and on a Siemens D-500 diffractometer, using Cu Kα radiation. The neutron diffraction patterns were acquired on the C2 Dualspec 800-wire high-resolution diffractometer with a wavelength of 1.3296 Å at Chalk River Laboratories (Ontario, Canada).

For the in situ X-ray diffraction measurements under hydrogen pressure, a small amount of Pd (2 wt %) was added to catalyze the dissociation of molecular hydrogen and to accelerate the kinetics of hydrogen intake by the B2 phase. As is well-known from the literature, most hydrogen-absorbing compounds must first be activated to show full hydrogen absorption capabilities. Usually, the activation procedure involves several high-temperature treatments which can alter the structure and phase composition of the material. To avoid such pitfalls, the use of a hydrogen dissociation catalyst (Pd) was preferred. This technique allows hydrogen absorption at room temperature in the as-produced state, with no need for any activation.[9] The added Pd catalyst (2 wt %) was dispersed on the surface of the powder, using a low-energy Fritsch Pulverizette 7. Following that, a small amount of W (10 wt %) was added by hand mixing to serve as an internal standard during the hydrogen absorption experiment. The in situ X-ray diffraction patterns were taken on a Philips X-PERT diffractometer equipped with a XRK-900 (Anton Paar) high-pressure and high-temperature cell. The experiments were performed in the following way. First, the X-ray diffraction pattern of the sample was recorded under He atmosphere at 70 °C. Hydrogen (8 atm) was then introduced in the cell and the sample was allowed to reach equilibrium during 15 min. A second X-ray diffraction pattern was then recorded while the sample was still exposed to hydrogen. Finally, hydrogen was evacuated from the cell and replaced by He at atmospheric pressure. Again, the sample was allowed to reach equilibrium during 15 min and a third diffraction pattern was recorded.

The Rietveld analyses were performed using GSAS,[10] a software which allows the simultaneous fitting of X-ray and

(6) Blouin, M.; Guay, D.; Schulz, R. *Nanostruct. Mater.* **1998**, *10*, 523.
(7) Blouin, M.; Guay, D.; Huot, J.; Schulz, R.; Swainson, I. P. *Chem. Mater.* **1998**, *10*, 3492.
(8) Blouin, M.; Guay, D.; Schulz, R. *J. Mater. Sci.*, accepted for publication.
(9) Zaluski, L.; Zaluska, A.; Tessier, P.; Ström-Olsen, J. O.; Schulz, R. *J. Alloys Compd.* **1995**, *217*, 295.
(10) Larson, A. C.; Von Dreele, R. B. GSAS−General Structure Analysis System, Los Alamos National Laboratory Report No. LAUR 86-748 1986.

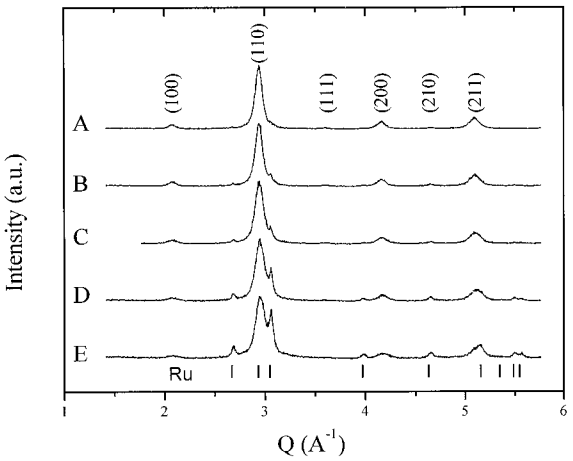

Figure 1. X-ray diffraction patterns of Ti:Ru:Fe ($2 - y$:$(1 + y)$/2:$(1 + y)$/2) powder mixtures milled for 40 h: (A) $y = 0.0$, (B) $y = 0.25$, (C) $y = 0.50$, (D) $y = 0.75$, and (E) $y = 1.0$. The peaks are indexed for the B2 cubic structure (cP2−CsCl).

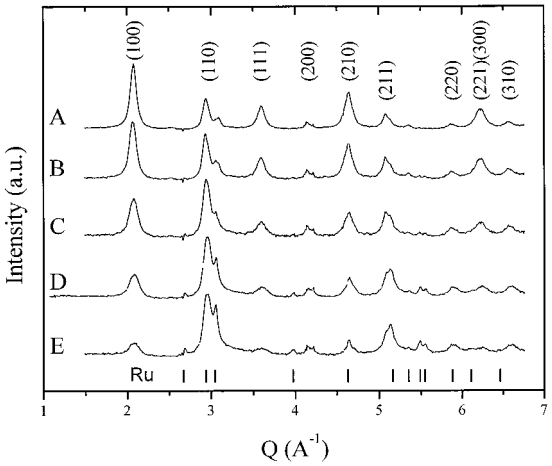

Figure 2. Neutron diffraction patterns of Ti:Ru:Fe ($2 - y$: $(1 + y)$/2:$(1 + y)$/2) powder mixtures milled for 40 h: (A) $y = 0.0$, (B) $y = 0.25$, (C) $y = 0.50$, (D) $y = 0.75$, (E) $y = 1.0$. The peaks are indexed for the B2 cubic structure (cP2−CsCl).

neutron diffractograms. The analyses were performed by using a modified pseudo-Voigt function, calibrated for instrumental broadening through the evaluation of standard powder histograms. For each sample, the value of the scale factor of the various phases was assumed to be identical for both histograms. Likewise, the values of the thermal parameters of the different atoms were the same for both the X-ray and neutron diffraction histograms. Soft chemical constraints were used to fix the chemical composition of the alloys during fitting. In the case of the cubic phase, 10 parameters were refined, namely the phase proportion and the lattice constant, two variables to define the peak shape (L_x and G_p) and three parameters (Ti, Ru, and Fe) for each of the two sites occupancies (1a and 1b). In the case of the minor phases (Fe, TiO, and Ru), only three parameters were refined, namely the phase proportion, the lattice constant, and one variable to define the peak shape (L_x). The parameters controlling the line profile of the minor phases were kept identical in the two histograms. The overall ratio R_{wp}/R_e of both histograms, with R_{wp} being the weighted profile difference between the calculated and measured intensities and R_e being an estimation of the minimum possible value of R_{wp}, was calculated. The value of R_{wp}/R_e is an indicator of the "goodness of the fit".

Results and Discussion

Structural Analyses of Nanocrystalline Ti:Ru:Fe. The X-ray and neutron diffraction histograms of nanocrystalline Ti:Ru:Fe ($2 - y$:$(1 + y)$/2:$(1 + y)$/2), with $y = 0.0$, 0.25, 0.50, 0.75, and 1.0, are shown in Figures 1 and 2, respectively. In these figures, the abscissa are expressed in Q units, with $Q = 4\pi \sin \theta/\lambda$. This has been done to take into account difference in the value of λ between the X-ray and the neutron radiation sources and to allow a direct comparison between the two histograms.

All X-ray histograms of Figure 1 exhibit the characteristic diffraction peaks of a simple B2 cubic phase (cP2−CsCl). The intensity ratio between any two of these peaks does not show any marked dependency on the Ti content. One can also notice the gradual appearance of the characteristic diffraction peaks of Ru (hP2−Mg) as the Ti content decreases from 2 to 1 (from curve A to curve E in Figure 1). The diffraction peaks are quite broad, indicating that these phases are present in the form of very small crystallites.

The neutron diffraction peaks belonging to the B2 cubic phase are also seen in Figure 2. In contrast to the X-ray diffraction, the intensity ratio of the peaks belonging to the B2 phase exhibits a marked dependency on the Ti content in the samples. For example, the intensity ratio of the (100) and (110) peak decreases steadily from a value larger than one for Ti:Ru:Fe (2:1:1), to a value smaller than unity for Ti:Ru:Fe (1:1.5:1.5). A variation in the intensity of the diffraction peaks of a given phase is indicative of a change in the stoichiometry of that phase.

The (100) diffraction peak of the B2 structure is a superlattice peak, whose intensity is proportional to the square of $([Ti]\times a6_{Ti} + [Fe]\times a6_{Fe} + [Ru]\times a6_{Ru})1a - ([Ti]\times a6_{Ti} + [Fe]\times a6_{Fe} + [Ru]\times a6_{Ru})1b$, where the [Ti], [Fe], and [Ru] are the concentrations of each species on the 1a and 1b sites, and the $\times a6$'s are the scattering factors of the various elements. In neutron scattering, $\times a6_{Fe} = 9.45 \times 10^{-15}$ m and $\times a6_{Ru} = 7.03 \times 10^{-15}$ m, while $\times a6_{Ti}$ is negative (-3.44×10^{-15} m).[11] So, depleting Ti from one site and replacing it by either Fe or Ru will have a marked effect on the intensity of the superlattice peaks of the neutron diffraction pattern. In the case of X-ray diffraction, the scattering factor ($\times a6$) is a function of the atomic number and thus, replacing Ti ($Z = 22$) by Fe ($Z = 26$) will not have a marked effect on intensities, while it will if Ti is replaced by Ru in the B2 structure. So, the fact that the intensity of the (100) peak is substantially affected in the neutron diffraction patterns and only marginally modified in the XRD patterns would tend to indicate a substitution of Ti by Fe in the B2 structure.

The neutron diffraction histograms of Figure 2 also show the gradual appearance of the characteristic diffraction peaks of Ru as the Ti content of the sample is reduced (from curve A to E). Also, consistent with what is observed in Figure 1, all the diffraction peaks are broad. For some samples, a weak (and sharp) peak is observed at $Q = 4.21$ Å^{-1}, which can originate from the V container used in the neutron diffraction measurements.

The histograms of each sample were analyzed using the Rietveld method to extract structural parameters. In each case, both X-ray and the neutron diffraction

(11) Sears, V. F. *Neutron News* **1992**, *3*, 26.

Table 1. Structural Parameters of the Milled Powders

samples Ti:Ru:Fe $(2-y{:}(1+y)/2{:}(1+y)/2)$	phases	phase proportion (wt %)	lattice parameters		crystal size		R_{wp}/R_e (%)
			a (Å)	c (Å)	X-ray (nm)	neutron (nm)	
$y = 0.00$	B2	97	3.025		11	8	1.26
	Fe	3	2.881		9	8	
$y = 0.25$	B2	92	3.023		13	9	1.27
	Fe	4	2.878		9	8	
	Ru	4	2.711	4.269	26	22	
$y = 0.50$	B2	92	3.020		11	10	1.37
	Fe	4	2.889		9	8	
	Ru	4	2.709	4.269	23	20	
$y = 0.75$	B2	77	3.012		10	10	1.28
	Ru	18	2.708	4.272	16	14	
	Fe	5	2.882		3	3	
$y = 1.00$	B2	69	3.005		10	10	1.36
	Ru	25	2.705	4.278	13	15	
	Fe	6	2.885		3	3	

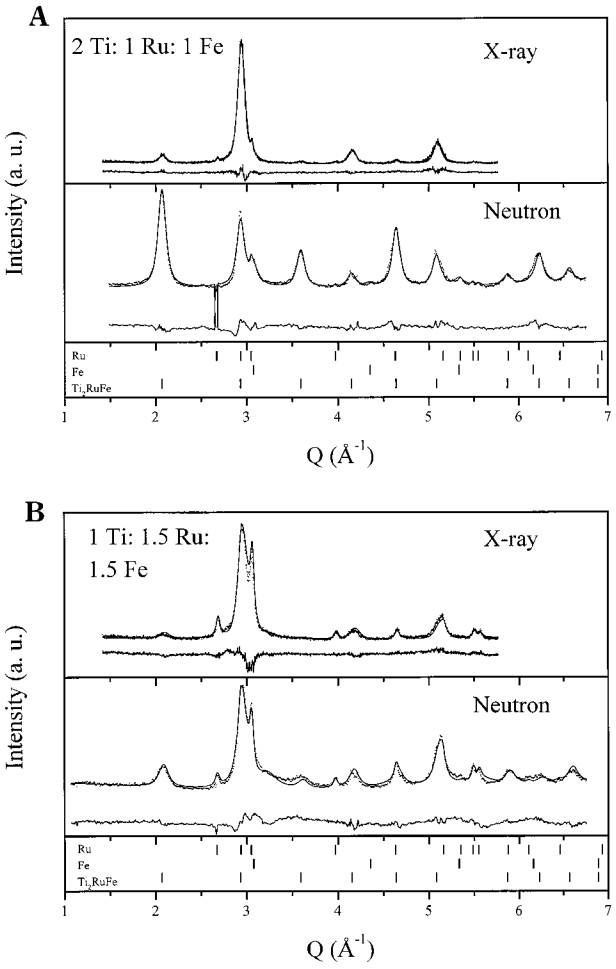

Figure 3. X-ray and neutron diffraction data of (A) Ti:Ru:Fe (2:1:1) and (B) Ti:Ru:Fe (1:1.5:1.5). The dots are the experimental data, while the full line is the simulated spectrum. Also shown is the difference curve between the experimental data and the simulated curve.

histograms were analyzed at the same time. The fitting parameters, namely the phase proportions, the lattice parameters and the crystallite size of each phase are given in Table 1. Two examples of the result of this analysis are shown for Ti:Ru:Fe (2:1:1) and (1:1.5:1.5) in parts A and B of Figure 3, respectively. In this figure, the dots are the experimental data points and the curve (full line) represents the calculated pattern. Also shown in these figures are the difference between the experimental and the calculated value.

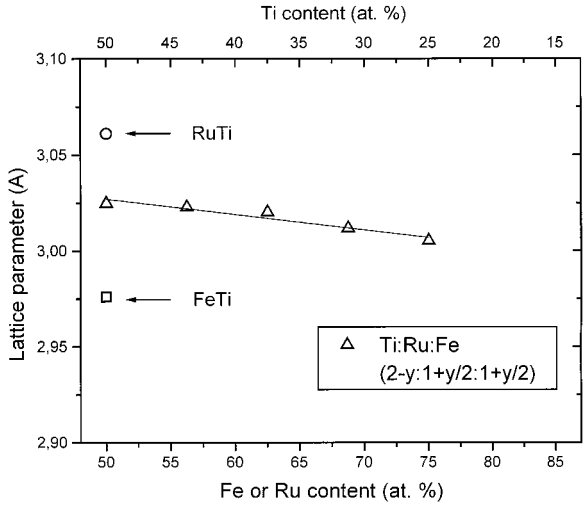

Figure 4. Variation of the lattice parameter of the B2 structure with respect to the Ti content of nanocrystalline Ti:Ru:Fe. Also shown are the lattice parameters of TiFe and TiRu.

In the case of Ti:Ru:Fe $(2-y{:}(1+y)/2{:}(1+y)/2)$ with $y = 0.00$, 0.25, and 0.50, the samples are made almost exclusively of the B2 cubic phase. In these samples, the phase proportion of Fe or Ru does not exceed 4 wt %. For samples with $y = 0.75$ and 1.00, the B2 phase proportion decreases to 77% and 69 wt %, respectively. In these last two samples, the phase proportion of Ru increases to 18 and 25 wt %, respectively.

The variation of the lattice parameter, a, of nanocrystalline Ti:Ru:Fe $(2-y{:}(1+y)/2{:}(1+y)/2)$ with the Ti content of the sample is depicted in Figure 4 (open triangles). For Ti:Ru:Fe (2:1:1), the value of a is almost at the midpoint between the values of TiFe (2.97 Å[12]) and TiRu (3.06 Å[13,14]). For samples with $y > 0.00$, the lattice parameter of the B2 phase decreases slowly as the Ti content is reduced. As far as the other phases are concerned, the lattice parameter of Fe is close to the tabulated value at 2.88 Å.[12] For Ru, while a is close to the tabulated value, c is slightly shorter (4.26 Å instead of 4.28 Å).[15] This is probably due to the presence of Fe solutes in the hcp structure of Ru. The crystallite size calculated from the parameters determining the

(12) *Pearson's Handbook of Crystallographic Data for Intermetallic Phases*; Villars, P., Calvert, L. D., Eds.; American Society for Metals: Materials Park, OH, 1985; Vol. 3
(13) Raub, V. E.; Röschel, E. *Z. Metallkd.* **1963**, *54*, 455.
(14) Jordan, C. B. *J. Metals* **1955**, *7*, 832.
(15) Raub, V. E.; Röschel, E. *Z. Metallkd.* **1960**, *51*, 477.

Table 2. Site Occupancies of the Simple Cubic Phases

samples Ti:Ru:Fe $(2-y):(1+y)/2:(1+y)/2)$	U_{iso}	site occupancy					
		1a site			1b site		
		Ti	Ru	Fe	Ti	Ru	Fe
$y = 0.00$	0.017	0.842	0.079	0.079	0.035	0.483	0.483
$y = 0.25$	0.018	0.796	0.000	0.204	0.000	0.445	0.555
$y = 0.50$	0.02	0.685	0.000	0.315	0.000	0.430	0.570
$y = 0.75$	0.024	0.602	0.000	0.398	0.000	0.511	0.489
$y = 1.00$	0.024	0.511	0.000	0.489	0.000	0.493	0.507

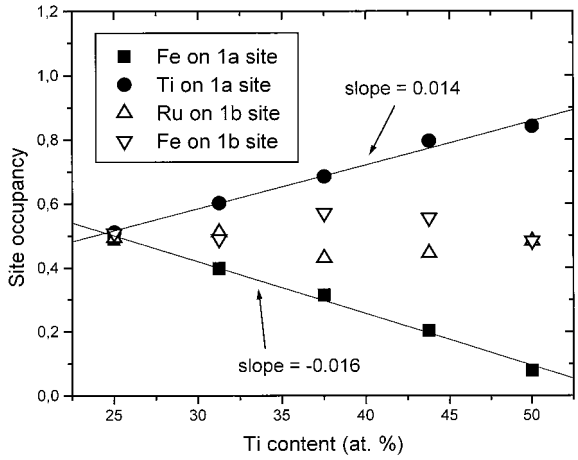

Figure 5. Variation of the site occupancies of the B2 structure with respect to the Ti content of nanocrystalline Ti:Ru:Fe.

line profile shape are all in the nanometer range. Except for Ru, which has a crystallite size around 25 nm, all other phases have crystallite size of the order of 10 nm. The parameters related to the strain were not fitted.

Other quantitative information extracted from the Rietveld refinement of the histograms is the site occupancies of each species in the unit cell of the B2 phase. This information is presented in Table 2. The B2 structure has two different sites: the 1a site which corresponds to the cube vertexes, and the 1b site located at the center of the cube. In the case of Ti:Ru:Fe (2:1:1), Ti occupies 84% of the 1a site, while Ru and Fe are found with an identical probability (48% each) on the 1b site. For that sample, a long-range order parameter, S, can be defined as $S = (x_{Ti} - F_{Ti})/(1 - F_{Ti})$, where x_{Ti} is the fraction of Ti sites occupied by Ti atoms and $F_{Ti} = 0.5$. The values of site occupancies found for Ti:Ru:Fe (2:1:1) yields to a S value of 0.68, close that determined previously for the same composition.[3,7]

The variation of the site occupancies for Ti, Ru, and Fe atoms with respect to the Ti content of the samples is shown in Figure 5. There is a marked decrease of the 1a site occupancy by Ti as the Ti content of the sample varies from 50 to 25 atom %. As evidenced by the data of Table 2, Ti atoms on the 1a site are replaced exclusively by Fe atoms. This is shown in Figure 5 by the fact that the regression lines going (i) through the Ti site occupancies on the 1a site (filled circles) and (ii) through the Fe site occupancies on the 1a site (filled squares), have almost equal but opposite slope. In contrast, there is almost no variation of either the Fe or the Ru site occupancies on the 1b site as the Ti content of the sample varies. Also, there is no evidence that Ti is found on the 1b site for Ti:Ru:Fe $(2-y):(1+y)/2:(1+y)/2)$ with $y \neq 0$. As a consequence of the preferential replacement of Ti by Fe, the extra Ru atoms added to compensate for the lower Ti content (y in Ti:Ru:Fe $(2-y):(1+y)/2:(1+y)/2)$ precipitate as an hexagonal phase. This explains the appearance of a Ru-like hcp phase in both the X-ray and neutron diffraction patterns as the Ti content of the sample is reduced.

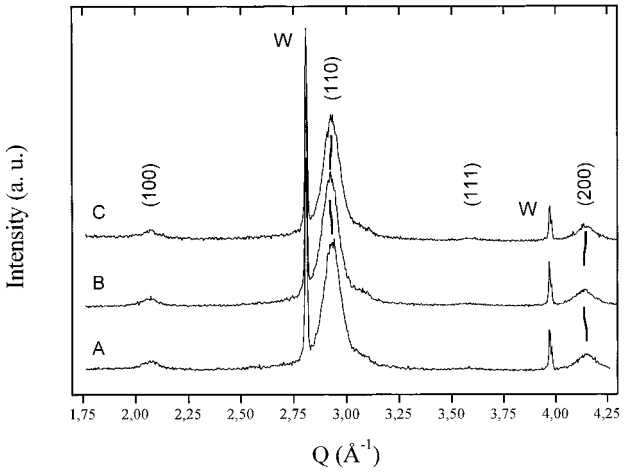

Figure 6. X-ray diffraction patterns of nanocrystalline Ti:Ru:Fe (2:1:1) recorded (A) before, (B) during, and (C) after exposure to hydrogen at high pressure (8 atm). The sample was prepared as described in the text.

It is interesting to compare the phases found in the nanocrystalline Ti:Ru:Fe $(2-y):(1+y)/2:(1+y)/2)$ samples with those formed at equilibrium in the binary Ti−Ru and Ti−Fe systems. The Ti−Ru binary phase diagram predicts the formation of a B2 structure near the equiatomic concentration, while a hcp-Ru like phase is obtained on the Ti-poor side of the phase diagram. The immiscibility gap between the B2 and the hcp phases is quite large, extending from $\sim 14 \leq [Ti] \leq \sim 48$ atom %. This means that the propensity of Ru atoms to occupy the 1a site of a B2 structure is quite low. This is consistent with the fact that Ru atoms do not replace Ti on the 1a site of the B2 phase in the nanocrystalline Ti:Ru:Fe $(2-y):(1+y)/2:(1+y)/2)$ compounds.

The phase diagram of the Ti−Fe binary system also predicts the formation of an equiatomic B2 structure for Ti concentration close to 50 atom %. However, and in contrast to the Ti−Ru case, a hcp-like $TiFe_2$ structure exists in the equilibrium phase diagram for [Ti] varying between ~28 and ~36 atom %. At still higher Fe concentrations, α-Fe is formed. So, in the case of Ti−Fe, the propensity of Fe atoms to sit on the 1a site of a B2 structure when $[Ti] \ll 50$ atom % is also low. No phase like $TiFe_2$ is found in the ball-milled nanocrystalline Ti:Ru:Fe $(2-y):(1+y)/2:(1+y)/2)$ compounds. Instead, a metastable B2 structure is formed, with Fe preferentially replacing Ti on the 1a site.

In Situ X-ray Diffraction under Hydrogen Pressure. In situ X-ray diffraction measurements under hydrogen at high pressure were performed on the various samples. The X-ray patterns recorded before (A), during (B), and after (C) exposure of nanocrystalline Ti:Ru:Fe (2:1:1) to hydrogen are shown in Figure 6.

Upon exposure to hydrogen, there is a small but noticeable change in the peak position of the B2 phase. The peaks are shifted to smaller Q values, indicating that there is an increase of the unit cell lattice parameter arising from the dissolution of hydrogen atoms into the cubic phase. As shown in Figure 6, this reaction is totally reversible and the diffraction peaks of the B2

Table 3. Lattice Parameters and Volume Variation upon Hydrogen Exposure

samples Ti:Ru:Fe $(2-y)$:$(1+y)/2$:$(1+y)/2$	as milled		under 8 atm H_2				amount of hydrogen absorbed per unit cell[a]
	lattice parameter (Å)	volume (Å^3)	lattice parameter (Å)	volume (Å^3)	Δa (Å)	ΔV (Å^3)	
$y = 0.0$	3.023	27.624	3.030	27.805	0.0066	0.181	0.072
$y = 0.25$	3.026	27.709	3.030	27.822	0.0041	0.113	0.045
$y = 0.50$	3.019	27.502	3.020	27.551	0.0018	0.049	0.020
$y = 0.75$	3.014	27.372	3.017	27.451	0.0029	0.079	0.032
FeTi	2.978						
RuTi	3.060						

[a] Calculated assuming that the change in the volume of the unit cell of the B2 structure following hydrogen absorption is 2.5 Å^3.

phase returns to their original values upon removal of hydrogen. In Figure 6, the (110) peak of the B2 phase varies from 2.930 (curve A or C) to 2.922 D^{-1} (curve B). For comparison, the main diffraction peak of W at 2.808 D^{-1} stay constant to within $\pm$ 0.001 D^{-1}, which is almost a factor of 10 smaller than the change observed in the (110) peak of the B2 phase upon hydryding. As far as we can tell from a comparison of curves A and C, there is no decomposition of the nanocrystalline Ti_2RuFe phase following hydriding. Similar experiments were conducted with the other nanocrystalline Ti:Ru:Fe $(2-y)$:$(1+y)/2$:$(1+y)/2$ samples with very similar results.

A Rietveld refinement analysis of each X-ray diffraction histograms was conducted to determine the lattice parameter, a, and the volume, a^3, of the unit cell of the B2 phase for the materials exposed to hydrogen at high pressure. For each sample, the parameters determined in the combined X-ray and neutron refinement procedure of the first part were used for site occupancies and thermal parameters. The results of the Rietveld refinements are summarized in Table 3.

As shown in Table 3, all nanocrystalline Ti:Ru:Fe samples exhibit a sizable increase of the lattice parameters of the B2 structure upon exposure to hydrogen, which reflects to the fact that hydrogen is absorbed into the structure of the material. The largest change (increase) of lattice parameter occurs for Ti:Ru:Fe $(2-y)$:$(1+y)/2$:$(1+y)/2$ with $y = 0.0$. The change in lattice parameter corresponds to a volume expansion of the unit cell of 0.181 Å^3. For y values larger than 0.0, the volume change decreases substantially. This smaller change in the lattice parameter indicates that less hydrogen is absorbed into the material.

An estimation of the amount of hydrogen dissolved into the material can be obtained if the volume expansion of the cubic unit cell upon hydrogen dissolution is known. In a CsCl-type structure (B2), the change in the volume of the unit cell due to the incorporation of one hydrogen atom is of the order of 2.5 Å^3.[16] Thus, a volume change of 0.181 Å^3 for Ti_2RuFe would indicate that 0.072 atom of hydrogen are absorbed per unit cell (or 0.144 atom of hydrogen per unit of structural formula Ti_2RuFe), which is in close agreement with what was found elsewhere from electrochemical measurements.[17] A similar calculation was performed for all nanocrystalline compounds and the results are shown in Table 3. It is clear that less hydrogen is absorbed as the Ti content of the B2 phase decreases.

According to Miedema,[18] the heat of formation of ternary hydrides AB_nH_{2m}, from the binary intermetallic compound AB_n and gaseous H_2 can be resolved into three contributions:

$$\Delta H(AB_nH_{2m}) = \Delta H(AH_m) + \Delta H(B_nH_m) - \Delta H(AB_n) \quad (1)$$

where A is Ti, B stands for an arbitrary transition metal, and n is assumed to be greater than one. For the purpose of the discussion, and to be able to rely on data already available in the literature, we will consider two limiting cases, namely those where B is either Ru or Fe, and where $m = {}^3/_2$. So, according to ref 18, the value of ΔH (TiH_2), which will appear in both calculations, is -30 kcal/mol TiH_2, while those of RuH and FeH are $+8$ and $+4$ kcal/mol, respectively. As expected, the values of ΔH (TiRu) and ΔH (TiFe) are negative. Thus, in the case of TiRu and TiFe, only the first term of eq 1 is negative and can contribute to the formation of stable ternary hydrides. This means that the stability of the hydride will decrease as the Ti content gets lower. It is interesting to note that this correlates with a decrease in the amount of hydrogen absorbed in the nanocrystalline Ti:Ru:Fe materials as the Ti content of the B2 phase diminishes.

Electrochemical Properties of Related Materials. These findings have some important consequences regarding the long-term stability of such materials when they are used to catalyze the hydrogen discharge reactions.

As shown elsewhere,[4] nanocrystalline Ti:Ru:Fe (2:1:1) electrodes are not stable in continuous hydrogen discharge conditions. This is even worse if the electrode is subjected to a succession of hydrogen discharge and open circuit conditions. It was hypothesized (i) that hydrogen dissolves into the structure of the B2 phase during hydrogen discharge and is released under open circuit conditions, and (ii) that the structural changes associated with the dissolution/release of hydrogen leads to the decrepitation and destruction of the electrode. The fact that a reversible change of the lattice parameter of the B2 phase is observed when the material is exposed to hydrogen at high pressure gives credit to this hypothesis.

Also, it is known that significant improvement of the long-term stability of nanocrystalline Ti:Ru:Fe (2:1:1) electrodes occurs by adding O.[4] As shown elsewhere,[6,7] apart from yielding to the formation of titanium oxides, the addition of O causes also the formation of a

(16) Westlake, D. G. *J. Less-Common Met.* **1983**, *90*, 251.
(17) Roué, L.; Guay, D.; Schulz, R. *J. Electroanal. Chem.*, in press.
(18) Miedema, A. R.; Buschow, K. H. J.; Van Mal, H. H. *J. Less-Common Met.* **1976**, *49*, 463.

Ti-depleted B2 phase. It was also hypothesized in ref 4 that these B2 phases with less Ti absorb less hydrogen and, therefore, are more resistant to decrepitation. The fact that the ΔV of the B2 structure become smaller as the Ti content decreases strongly supports this idea.

The next step in demonstrating the soundness of the previous hypothesis is to directly test the long-term stability of nanocrystalline Ti:Ru:Fe $(2 - y):(1 + y)/2:(1 + y)/2)$ material electrodes. As shown elsewhere,[19] an improvement in the stability of nanocrystalline Ti:Ru:Fe $(2 - y):(1 + y)/2:(1 + y)/2)$ under conditions where hydrogen is evolved from the electrodes is observed for $y > 0$. Moreover, the level of improvement is dependent on the value of y, increasing as y varies from 0 to 0.75. These results, which are presented in full details elsewhere,[19] give further strength to the hypothesis presented above.

Conclusion

It was shown that a Ti-depleted B2 cubic phase can be formed directly by high-energy ball milling, starting from a powder mixture of Ti, Ru, and Fe. The occurrence of such a Ti-depleted B2 phase has already been evidenced in nanocrystalline Ti:Ru:Fe:O compounds.[7]

Using in situ X-ray diffraction measurements under hydrogen at high pressure, it was shown that there is a noticeable increase of the lattice parameter of the B2 phase of nanocrystalline Ti:Ru:Fe $(2 - y):(1 + y)/2:(1 + y)/2)$ upon exposure to hydrogen. This increase is reversible when hydrogen is removed from the cell. It was also shown that the Δa and ΔV values decrease as the Ti content of the B2 phase diminishes, indicating that the amount of hydrogen absorbed decreases as the Ti content decreases.

An important factor influencing the propensity of nanocrystalline Ti:Ru:Fe materials to form a hydride is the amount of Ti. Therefore, nanocrystalline Ti:Ru:Fe with decreasing Ti content will be more resistant to hydride formation.

Acknowledgment. This work was supported by the Natural Sciences and Engineering Research Council of Canada and Hydro-Québec.

CM990293Z

(19) Roué, L.; Bonneau, M.-E.; Guay, D.; Blouin, M.; Schulz, R. *J. Appl. Electrochem.*, in press.